Int. J. Therm. Sci. (2001) 40, 816–824

S1290-0729(01)01268-6/FLA

Developing mixed convection with aiding buoyancy in vertical tubes: a numerical investigation of different flow regimes

Maher Zghal [a1], Nicolas Galanis [a*], Cong Tam Nguyen [b]

[a] *Faculté de génie, Université de Sherbrooke, Sherbrooke, QC, Canada*

[b] *École de génie, Université de Moncton, Moncton, NB, Canada*

(Received 2 June 2000, accepted 8 December 2000)

Abstract — Laminar upward flows with mixed convection in a vertical tube with a uniformly heated zone preceded and followed by adiabatic zones were investigated numerically. Calculations were performed by solving the elliptic Navier–Stokes and energy equations for air and a wide range of heating lengths, Reynolds and Richardson numbers. Different combinations of these parameters establish the existence of five types of flow fields: developing with or without flow reversal, developing followed by a fully developed region both without flow reversal, and developing with flow reversal followed by a fully developed region with or without flow reversal. The conditions leading to flow reversal as well as significant upstream diffusion of heat and momentum have been mapped on the Peclet–Richardson plane for different lengths of the heated zone. © 2001 Éditions scientifiques et médicales Elsevier SAS

mixed convection / elliptic model / flow regimes / upstream diffusion / flow reversal / effects of heating length

Résumé — **Convection mixte à l'entrée d'un tube vertical chauffée : étude numérique des différents régimes d'écoulements.** L'écoulement laminaire ascendant dans un tube vertical chauffé uniformément sur une partie de sa longueur a été étudié numériquement. Les résultats ont été obtenus en solutionnant les équations elliptiques, couplées, non linéaires de Navier–Stokes, de continuité et de conservation d'énergie pour l'air et plusieurs valeurs de la longueur de chauffage, du nombre de Reynolds et du nombre de Richardson. Ces paramètres déterminent le régime d'écoulement qui peut être : en développement avec ou sans renversement, en développement suivi d'une zone hydrodynamiquement et thermiquement développée sans renversement, ou bien en développement avec renversement suivi d'une zone hydrodynamiquement et thermiquement développée avec ou sans renversement. Les conditions qui engendrent le renversement et celles qui correspondent à une importante diffusion axiale de chaleur et/ou de la quantité du mouvement sont identifiées sur le plan Péclet–Richardson pour différentes longueurs de la section de chauffage. © 2001 Éditions scientifiques et médicales Elsevier SAS

convection mixte / modèle elliptique / régimes d'écoulement / diffusion axiale / renversement de l'écoulement / effets de la longueur de chauffage

Nomenclature

c_p	specific heat of the fluid	$J \cdot kg^{-1} \cdot K^{-1}$
D	internal tube diameter	m
g	gravitational acceleration	$m \cdot s^{-2}$
Gr	Grashof number $= \rho^2 g \beta q'' D^4 \mu^{-2} k^{-1}$	
h	convection heat transfer coefficient	$W \cdot m^{-2} \cdot K^{-1}$
k	thermal conductivity of the fluid	$W \cdot m^{-1} \cdot K^{-1}$
L_1, L_3	lengths of adiabatic zones	m
L_2	length of heated zone	m
Nu	Nusselt number $= hD/k$	
p	pressure	Pa
Pe	Péclet number $= Pr\,Re$	
Pr	Prandtl number $= c_p \mu / k$	
q''	heat flux	$W \cdot m^{-2}$
r, z	dimensionless radial and axial coordinates	
R, Z	radial and axial coordinates	m
Re	Reynolds number $= \rho V_0 D / \mu$	
Ri	Richardson number $= Gr/Re^2$	
T	temperature	K
T_0	fluid temperature at the tube entrance	K
V_0	average axial velocity	$m \cdot s^{-1}$
v_r, v_z	radial and axial velocity components	$m \cdot s^{-1}$

* Correspondance and reprints.

E-mail addresses: nicolas.galanis@gme.usherb.ca (N. Galanis), nguyenc@umoncton.ca (C.T. Nguyen).

[1] Presently with EMCO Ltd., Montréal, QC, Canada.

V_r, V_z dimensionless velocity components

Greek letters

β	thermal expansion coefficient	K^{-1}
θ	dimensionless temperature	
μ	dynamic viscosity	$kg \cdot m^{-1} \cdot s^{-1}$
ρ	density	$kg \cdot m^{-3}$
φ	tangential coordinate	

1. INTRODUCTION

Mixed convection in ducts occurs when a moving fluid is heated or cooled. It is encountered in many engineering applications such as heat exchangers, nuclear reactors, solar collectors, etc. In order to design such apparatuses and to predict their off design performance, it is necessary to obtain an exact description of the velocity, pressure and temperature distributions under all operating conditions.

To achieve this goal the fluid is practically always considered to be Newtonian and is modeled using the Boussinesq hypothesis. For steady state laminar flow the hydrodynamic and temperature fields are completely described by the five partial differential equations expressing conservation of mass, energy and momentum. These equations are non-linear, elliptic in all three directions and coupled because of the buoyancy force created by the temperature gradient. An analytical solution has been obtained for fully developed conditions [1] but the entire flow field can only be determined numerically.

The problem has been studied for isothermal ducts [2], and for uniform [3] or non-uniform [4] heat flux conditions. In these three studies, and in most of the other numerical studies of mixed convection in ducts, the length of the heat transfer zone is assumed to be infinite. In the few cases where this length has been assumed to be finite [5, 6] it has been assigned a single fixed value. Therefore the effects of this parameter on the hydrodynamic and thermal fields have not been investigated. A first objective of the present study is to evaluate these effects.

The boundary conditions at the inlet are almost always applied at the beginning of the heat transfer zone [2, 4] although it has been argued [7] that they should be applied further upstream to account for the possible effects of upstream diffusion. In the case of isothermal flows, momentum axial diffusion can be neglected far from the immediate entrance provided the Reynolds number is greater than approximately 400 [7]. In the case of forced convection with simultaneously developing hydrodynamic and thermal fields it has been shown [8] that a general criterion for the consideration of the axial diffusion terms should include both the Reynolds and Prandtl numbers. Finally, in the case of mixed convection it has been shown [6] that for air and one particular heating zone length, the importance of upstream diffusion of heat and momentum depends on the Reynolds and Grashof numbers. Unfortunately, the results in [6] are of limited practical interest since they were calculated for one very short length of the heating zone (10 diameters). A second objective of the present study is to generalize these results.

Boundary conditions at the duct outlet are usually chosen by assuming that the heat transfer zone is infinitely long and that the corresponding hydrodynamic and thermal fields are fully developed. For the case of an isothermal solid-fluid interface this condition is acceptable since the fluid eventually reaches a uniform temperature and the effects of buoyancy disappear. On the other hand, for a uniform heat flux applied at an infinitely long interface, the fully developed condition is questionable since it has been shown that the flow can become unstable if it is heated over a very long distance [9, 10]. Many numerical studies of mixed convection avoid this difficulty by neglecting axial diffusion of heat and momentum as proposed by Patankar and Spalding [11]. Thus the equations become parabolic in the axial direction and the need for boundary conditions at the duct outlet is eliminated. Furthermore, in this case the numerical solution becomes easier, since it is possible to use a marching technique in the axial direction, and the required computer memory is considerably reduced. However, this approach can not predict flow reversal which has been observed experimentally [10] and calculated with the fully elliptic model [6].

In view of these comments and the stated objectives, the present study has used the elliptic formulation to determine the hydrodynamic and thermal fields for upward flow of air in a long circular duct with uniform heat flux over a finite length. Velocity and temperature profiles were calculated in the heating zone, as well as in the adiabatic zones which precede and follow it, for Reynolds numbers up to 600, Grashof numbers up to 10^6 and heating lengths between 10 and 50 tube diameters. These results show the effects of *Re*, *Gr* and the heating length on the existence of fully developed flow and flow reversal as well as on the importance of upstream diffusion. Therefore they can be used to determine whether the axially parabolic formulation can be used to model the flow. As noted earlier, the effects of the heating zone length on these flow characteristics have not been reported up until now in the literature.

2. MATHEMATICAL FORMULATION AND NUMERICAL SCHEME

The system under consideration is shown in *figure 1*. The fluid enters a vertical circular duct of internal diameter D at $Z = -L_1$ with uniform temperature T_0. A uniform heat flux q'' is imposed at the solid-fluid interface from $Z = 0$ to $Z = L_2$ while the rest of the interface is adiabatic. The following assumptions are used:

- The fluid is Newtonian and incompressible; its properties are constant, except for the density whose variation is considered only in the buoyancy terms and modeled using the Boussinesq approximation.
- The flow is laminar, steady, two-dimensional ($\partial/\partial\varphi = 0$) and viscous dissipation is negligible.
- The wall thickness is very small compared to the tube diameter; thus, the thermal boundary condition on the lateral surface is applied at the solid-fluid interface:

at $R = D/2$:

$$\begin{aligned} &V_z = V_r = 0 \\ &\partial T/\partial R = q''/k, \quad \text{for } 0 \le Z \le L_2 \\ &\partial T/\partial R = 0, \quad \text{elsewhere} \end{aligned} \tag{1}$$

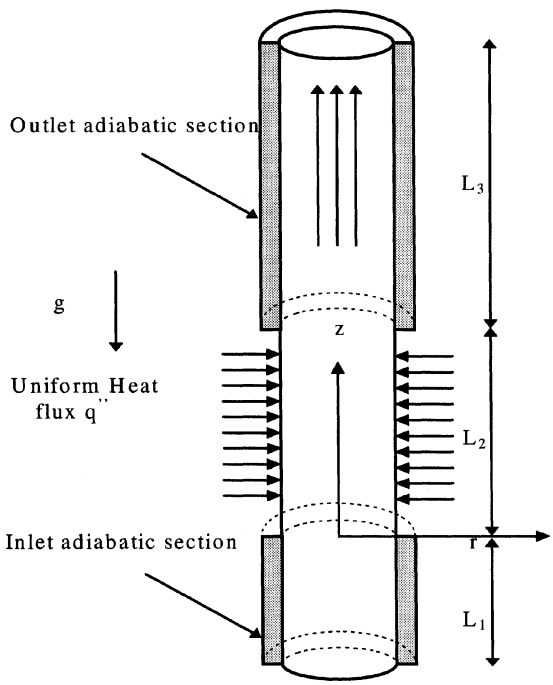

Figure 1. Schematic representation of system under study.

- The inlet adiabatic zone is used to avoid any interference between the corresponding boundary conditions and an eventually important upstream diffusion of heat and momentum. Thus

at $Z = -L_1$:

$$V_r = 0, \qquad T = T_0, \qquad V_z = 2V_0\left(1 - 4(r/D)^2\right) \tag{2}$$

Non dimensional quantities are obtained by using the diameter D, the average axial velocity V_0, $\rho(V_0)^2$ and $q''D/k$ as reference quantities for lengths, velocities, pressure and temperature difference $(T - T_0)$, respectively. Therefore, the thermo-hydrodynamic evolution is modeled by the following non-dimensional form of the governing equations:

$$\left(\frac{\partial v_r}{\partial r} + \frac{v_r}{r}\right) + \frac{\partial v_z}{\partial z} = 0 \tag{3}$$

$$v_r\frac{\partial v_r}{\partial r} + v_z\frac{\partial v_r}{\partial z} = -\frac{\partial p}{\partial r} + \frac{1}{Re}\left[\frac{1}{r}\frac{\partial}{\partial r}\left(r\frac{\partial v_r}{\partial r}\right) + \frac{\partial^2 v_r}{\partial z^2} - \frac{v_r}{r^2}\right] \tag{4}$$

$$v_r\frac{\partial v_z}{\partial r} + v_z\frac{\partial v_z}{\partial z} = \frac{Gr}{Re^2}\theta - \frac{\partial p}{\partial z} + \frac{1}{Re}\left[\frac{1}{r}\frac{\partial}{\partial r}\left(r\frac{\partial v_z}{\partial r}\right) + \frac{\partial^2 v_z}{\partial z^2}\right] \tag{5}$$

$$v_r\frac{\partial \theta}{\partial r} + v_z\frac{\partial \theta}{\partial z} = \frac{1}{Pe}\left[\frac{1}{r}\frac{\partial}{\partial r}\left(r\frac{\partial \theta}{\partial r}\right) + \frac{\partial^2 \theta}{\partial z^2}\right] \tag{6}$$

This elliptical formulation necessitates boundary conditions at the exit of the domain. A long adiabatic zone was therefore added downstream of the heated region to allow the use of fully developed conditions:

at $Z = L_2 + L_3$:

$$\partial V_r/\partial Z = \partial V_z/\partial Z = \partial T/\partial Z = 0 \tag{7}$$

Equations (3)–(6) indicate that the flow field depends on the values of three non-dimensional parameters: the Prandtl, Reynolds and Grashof numbers or, equivalently, the Prandtl, Péclet and Richardson numbers. This system of coupled, non-linear, elliptic partial differential equations is solved using the finite volume method. The equations are integrated over a control volume and discretized. By assuming a pressure distribution it is then possible to calculate the velocity components and the temperature from the momentum and energy equations. In general, these velocity components do not satisfy the equation of continuity. It is therefore necessary to proceed by iteration: the pressure field is corrected using the integrated

expression of mass conservation and the SIMPLEC algorithm [12] is used to obtain the corrected velocity components. Under-relaxation is used during the iterative procedure while the convergence criterion is based on the mass residual.

The discretization grid is based on a power law for the radial direction and on a geometric series progression in the axial direction. They result in a higher density of grid points in the regions where the gradients of velocity and temperature are more important. Several different grids were tested to ensure that the results are grid-independent [13]. The one finally adopted consists of 20 radial nodes and 400 to 600 axial nodes depending on the length of the heated zone. Similarly, calculations were also performed with different values of the convergence criterion (different mass residuals) to ensure that its value did not influence the results [13]. The average false diffusion coefficient has been estimated to be less than 1% of the real diffusion coefficients for both heat and momentum transfer in all the cases studied.

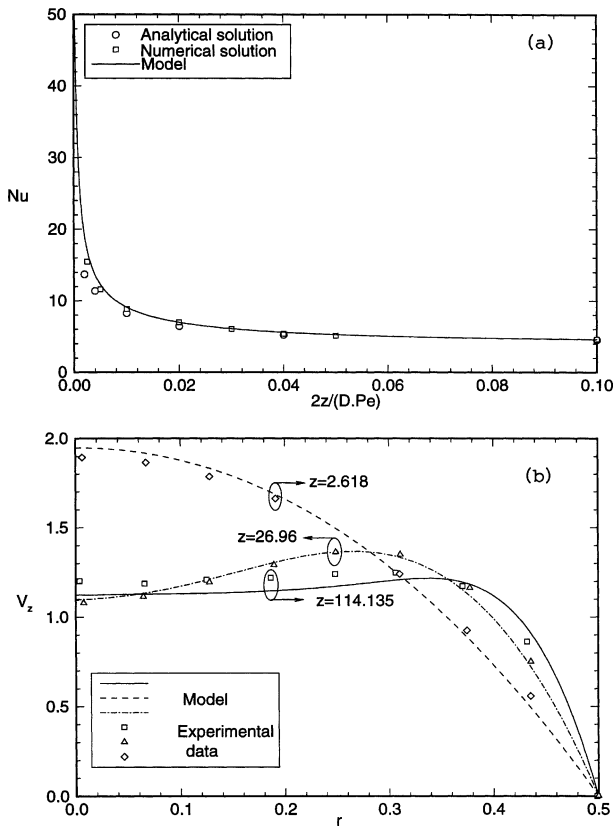

Figure 2. Validation of the computer code for (a) forced connection, and (b) mixed convection.

The computer code was validated by comparing its predictions with analytical, numerical and experimental results. *Figure 2(a)* shows a comparison of our calculated values for the axial evolution of the local Nusselt number for forced convection with the corresponding analytical solution [14] and the numerical results given by Kays [15]. The small differences between the analytical and numerical results close to the tube entrance are due to the use of only five terms of the infinite series analytical solution. *Figure 2(b)* shows a comparison of our calculated axial velocity profile for mixed convection with the corresponding experimental results by Zeldin and Schmidt [16]. The agreement between our results and those obtained by other methods in these and other cases [13] shows that the model is satisfactory and the computer code is reliable. They can therefore be used with confidence for the study of the problem under consideration.

3. RESULTS AND DISCUSSION

3.1. Field description for a representative case ($Pr = 0.7$, $Re = 500$, $Ri = 4$)

Previous results [6, 10] have shown that for ascending heated flow the acceleration due to buoyancy can result in an axial velocity profile which exhibits a maximum value elsewhere than at the tube axis ($r = 0$). Furthermore, the velocity at, and near, the tube axis may become negative. These studies have also shown that the onset of this flow reversal depends on the values of the Prandtl, Péclet and Richardson numbers. *Figure 3*, which shows the evolution of the axial velocity at $r = 0$ for four different heating lengths L_2, indicates that the onset of flow reversal also depends on the value of this last parameter. Indeed, the minimum velocity for $L_2 = 10$ is positive (no flow reversal) while it is negative (flow reversal is present) for the three longer heating zones. Based on the references reviewed in this and our previous articles on mixed convection [4, 6, 17] this effect of the heating length has never been reported before.

Figure 3 also shows that for all four cases the axial velocity at $r = 0$ decreases rapidly in the heating zone. For $L_2 = 10$ it reaches its minimum value just beyond the end of the heating zone. For the three longer heating zones the minimum is identical and it occurs at the same axial position ($z = 14$). Beyond the minimum, the axial velocity for the two shorter heating zones ($L_2 = 10$ and $L_2 = 15$) increases monotonically towards 2.0 since heat

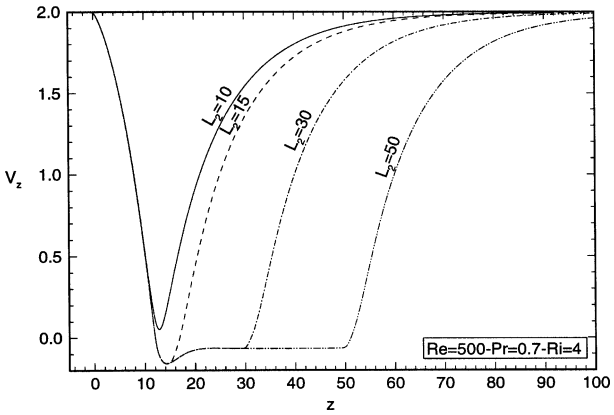

Figure 3. Evolution of the axial velocity at $z = 0$.

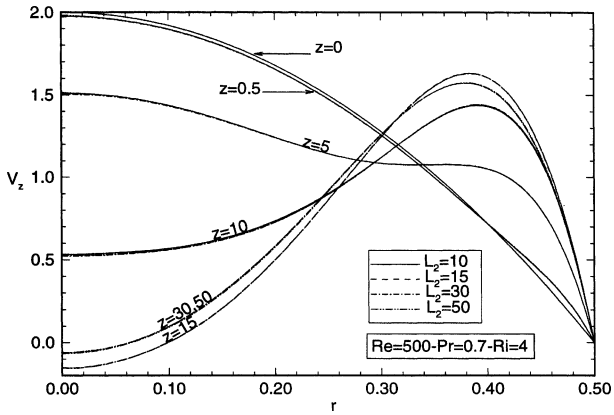

Figure 4. Evolution of axial velocity profile.

is not supplied any longer and the velocity profile in the outlet adiabatic zone tends towards the parabolic Poiseuille radial distribution. On the other hand, for $z > 14$, the velocities for the two longer heating zones ($L_2 = 30$ and $L_2 = 50$) increase slightly and attain a constant negative value from $z \approx 21$ to the end of the heating zone. The asymptotic tendency beyond this point is identical to the one for the two shorter heating zones.

The fact that the centerline axial velocity for the two longer heating zones remains constant over a certain distance suggests the existence of a hydrodynamically fully developed region. *Figure 4* substantiates this suggestion since the velocity profiles at $z = 30$ and $z = 50$ are exactly the same for $L_2 = 50$. In fact, this velocity profile applies everywhere beyond $z \approx 21$ to the end of the heated zone for both $L_2 = 50$ and $L_2 = 30$. *Figure 4* also shows that, for the present combination of flow parameters, the velocity profiles from $z = 0$ to the end of the heating zone are identical for all values of L_2. Thus, for example, the velocity profiles for $L_2 = 18$ would be the same as those for $L_2 \geq 18$ for any axial position between $z = 0$ and $z = 18$.

The results of *figure 4* also show that the velocity profile at the entrance of the heating zone ($z = 0$) is parabolic, i.e., identical to the one imposed at $z = -L_1$. Therefore, for the flow parameters under consideration, upstream diffusion of momentum towards the inlet adiabatic zone is negligible. Further downstream, the axial velocity profile becomes flatter and, eventually, the maximum velocity occurs fairly close to the fluid-solid interface due to the buoyancy induced acceleration.

The corresponding temperature profiles are shown in *figure 5*. It should be noted that, for the combination of flow parameters under consideration, the temperature profile at the entrance of the heating zone ($z = 0$) is

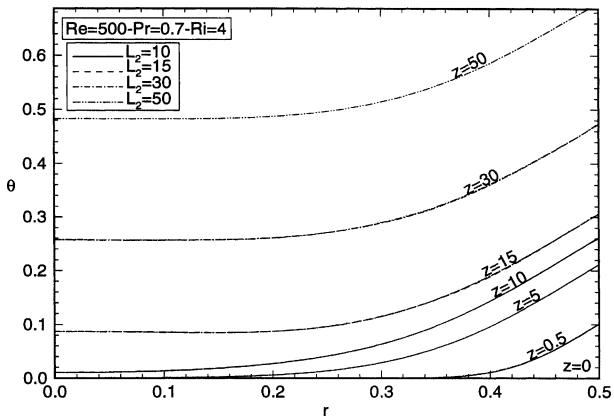

Figure 5. Evolution of temperature profile.

identical to the inlet condition imposed at $z = -L_1$. Thus, in this case, upstream heat diffusion towards the inlet adiabatic zone is negligible. Similarly to the velocity profiles, we note that the temperature profiles up to the end of the heating zone are identical for all values of L_2. Thus, for example, the temperature profiles for $L_2 = 18$ would be the same as those for $L_2 > 18$ for any axial position between $z = 0$ and $z = 18$. *Figure 6* which shows the axial evolution of the difference between the fluid bulk temperature and the wall temperature establishes the existence of a thermally developed field beyond $z \approx 21$ for the two longer heating zones ($L_2 = 30$ and $L_2 = 50$). Indeed, beyond this position that temperature difference remains constant. It should also be noted that it has the same value for both $L_2 = 30$ and $L_2 = 50$ in accordance with the corresponding observation regarding the temperature profiles in *figure 5*.

Figures 7 and *8* show the evolutions of the resistance coefficient and the local Nusselt number respectively.

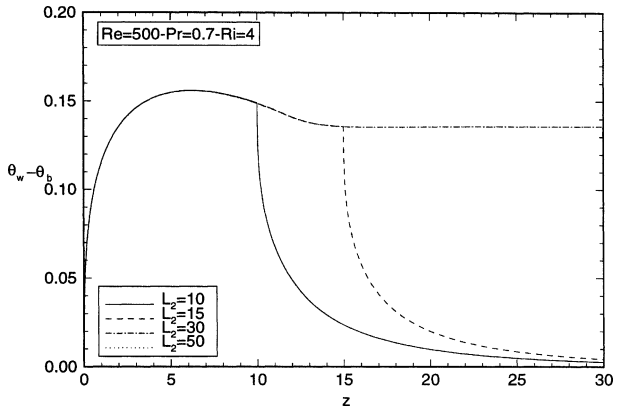

Figure 6. Difference between fluid bulk and wall temperatures.

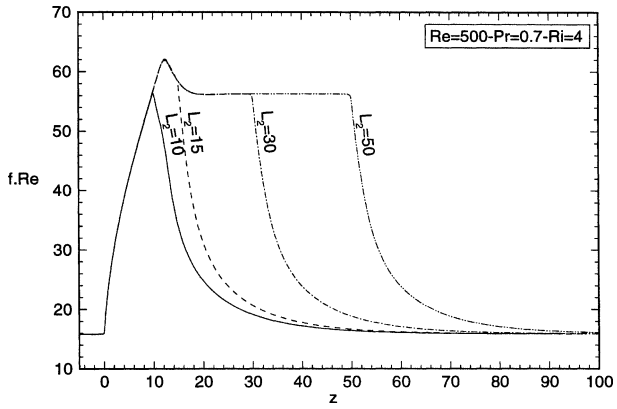

Figure 7. Evolution of the resistance coefficient.

Very close to the beginning of the heated zone these two variables are essentially identical to the corresponding values for forced convection since the buoyancy induced acceleration has not yet manifested itself. Further downstream however, their values are greater than the corresponding ones for forced convection which are, for fully developed conditions, $(fRe)_\infty = 16$ and $Nu_\infty = 4.36$. The results of these figures confirm two previous conclusions:

(a) the existence of a fully developed region for $21 < z < L_2$ in the case of the two longer heating zones, and

(b) the fact that, for the flow parameters under consideration, the hydrodynamic and thermal variables at any cross section up to the end of the heating zone are identical for all values of L_2.

Finally, *figure 9* shows the streamlines for each of these four cases (it should be noted that in this figure radial dimensions are 29 times greater than axial dimensions). This representation of the flow field clearly shows the regions of developing (axially dependent) and hydro-

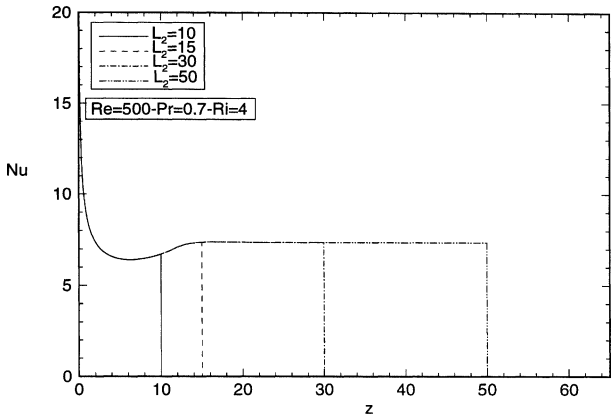

Figure 8. Evolution of local Nusselt number.

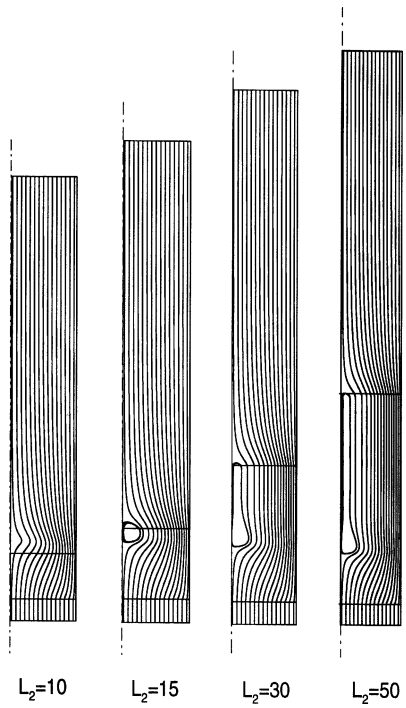

Figure 9. Streamlines for different values of L_2 ($Pr = 0.7$, $Re = 500$, $R = 4$).

dynamically developed (axially independent) flow: in the former the streamlines are curved while in the latter they are parallel to the tube axis. The shape of the recirculation bubble, associated with the region of negative axial velocity at $r = 0$, is clearly visible for the three longer heating zones. For $L_2 = 15$ the cross section of the recirculation bubble is very nearly elliptical. On the other hand, for the longer heating zones the radial dimension of the recirculation bubble grows from zero to a maximum

value, decreases slightly and remains constant until the end of the heating zone. It is therefore possible to identify three different flow regimes in the heating zones for the flow conditions under consideration.

(a) A developing flow without flow reversal (for $L_2 = 10$).

(b) A developing flow with flow reversal (for $L_2 = 15$).

(c) A hydrodynamically developing flow with flow reversal followed by a developed flow with flow reversal (for $L_2 = 30$ and $L_2 = 50$). According to the previous observations regarding *figures 5, 6* and *8* the flow field is also thermally developed in this part of the heating zone.

3.2. Effects of the Reynolds and Richardson numbers

Contrary to the results of *figures 4* and *5*, those in *figures 10* and *11* show that the effects of upstream diffusion are significant when the Reynolds number decreases and/or when the Richardson number increases. Indeed, these results show that at $z = 0$ the fluid near the fluid-solid interface is considerably warmer than at $z = -L_1$, and that the corresponding axial velocity profile is significantly distorted because of the resulting buoyancy force. In such cases the application of the inlet boundary conditions at the beginning of the heated zone ($z = 0$) is obviously not acceptable since it would result in a distortion of the flow field.

Figure 12 shows the effect of the Richardson number on the streamlines. When these patterns for $L_2 = 50$ are compared with the corresponding one in *figure 9*, we note that as *Ri* decreases from 4 to 3.4 the size of the recirculation bubble decreases as well. When *Ri* decreases even further ($Ri = 1$) there is no recirculation at all (flow reversal does not occur for this combination of flow variables). The evolution of the velocity and temperature profiles for these two cases (not reproduced here for the sake of brevity) shows similarities and differences from those presented in *figures 3–8*. Thus:

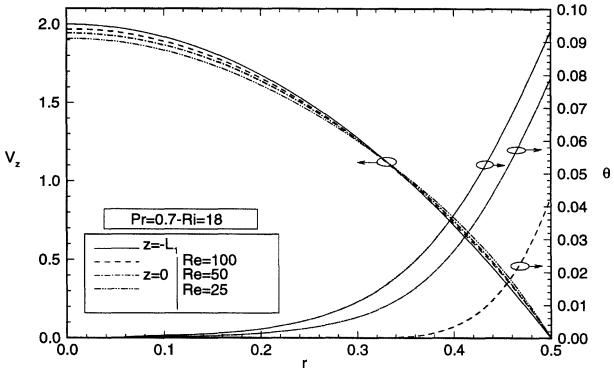

Figure 10. Effect of *Re* on axial velocity and temperature profiles.

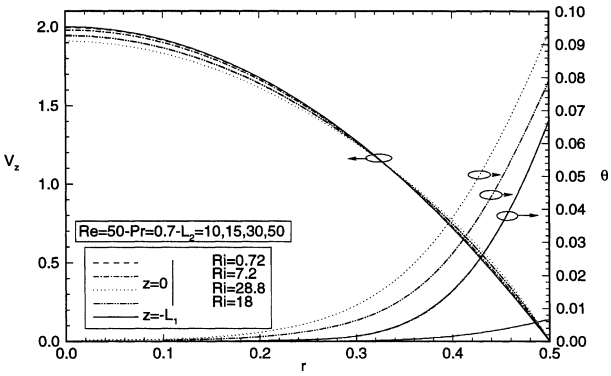

Figure 11. Effect of *Ri* on axial velocity and temperature profiles.

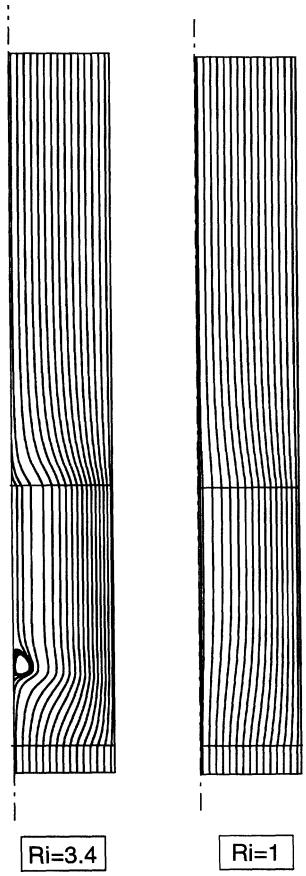

Figure 12. Streamlines for different values of *Ri* ($Pr = 0.7$, $Re = 500$, $L_2 = 50$).

– For $Ri = 3.4$ the axial velocity at $z = 0$ decreases rapidly in the heating zone and reaches a negative minimum at $z \approx 15$. It then increases slightly to a positive value which remains constant for $23 < z < 50$. This last result indicates that the flow is hydrodynamically developed in the downstream region of the heating zone, a fact confirmed by the axial velocity profiles which are identical throughout this region. Since the temperature is found to increase linearly in this region, the corresponding flow field is fully developed. The fundamental difference from the results presented in *figures 3–8* is that in the present case this fully developed flow is not concurrent with flow reversal. Therefore this flow regime is different from the three identified at the end of the previous section.

– For $Ri = 1$ the axial velocity at $z = 0$ decreases rather slowly in the heating zone and reaches a positive minimum at $z \approx 30$ (no flow reversal). It then remains constant until the end of the heated zone. Once again this suggests that the flow is hydrodynamically developed, a fact which is confirmed by the axial velocity profiles which are invariable in this region. Since the temperature in this region increases linearly with z, the flow field is also thermally developed. This flow field, which consists of a developing and fully developed region, both without flow reversal, is different from all four previously described.

3.3. Synthesis and decision charts

The previous results have established that certain combinations of *Pr*, *Pe*, *Ri* and L_2 can result in flow reversal. *Figure 13* presents the critical combinations of these variables for $Pr = 0.7$. In general, for given values of *Pr*, *Pe* and L_2 the critical value of *Ri* depends on both *Pe* and L_2. However, for any given value of *Pe* there exists a characteristic length L_u such that for $L_2 > L_u$ the critical value of *Ri* depends only on *Pe*; as shown in the figure this characteristic length increases linearly with *Pe*. Furthermore, for any given value of L_2 there exists an asymptotic value Ri_∞ such that for $Ri < Ri_\infty$, flow reversal does not occur for any values of *Pe*. It is obvious that the elliptic model must be used for any combination of flow parameters for which flow reversal occurs. It should even be used when flow reversal does not occur but the combination of flow parameters is close to the critical conditions. The axially parabolic model can be used only if the combination of flow parameters is well removed from the critical conditions.

Figures 10 and *11* have shown that when the Reynolds number is small and the Richardson number is large, upstream diffusion of heat and momentum results in significant changes of the velocity and temperature profiles between $z = -L_1$ and $z = 0$. When this happens, the inlet boundary conditions cannot be applied at the beginning of the heating region. In order to quantify these changes we have expressed the difference between corresponding values of $V_Z(r)$ and $\theta(r)$ at $z = -L_1$ and $z = 0$ as a percentage of the former. *Figure 14* shows the combinations of flow conditions which result in significant ($> 2\%$) or small ($< 2\%$) changes in these two profiles for $Pr = 0.7$. We note that, for a given Péclet number, significant changes in the velocity profile occur for smaller values of the Richardson number than those leading to significant changes in the temperature profile. The inlet boundary conditions (parabolic velocity profile, uniform temperature profile) can be applied at the beginning of the heating region only when the Richardson number is quite small ($Ri < 2$ for $Pe = 20$ and $Ri < 0.6$ for $Pe = 70$). For higher Péclet numbers an upstream adiabatic region should always be included in the calculation domain.

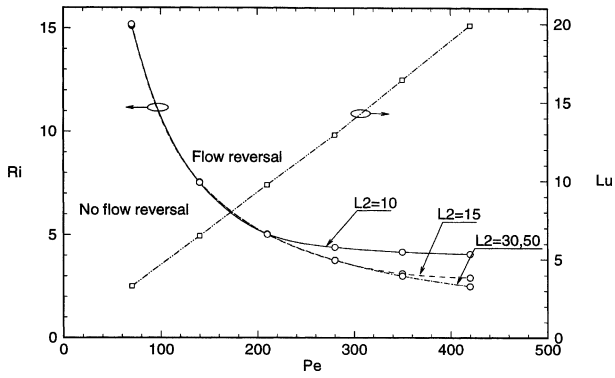

Figure 13. Flow reversal chart for $Pr = 0.7$.

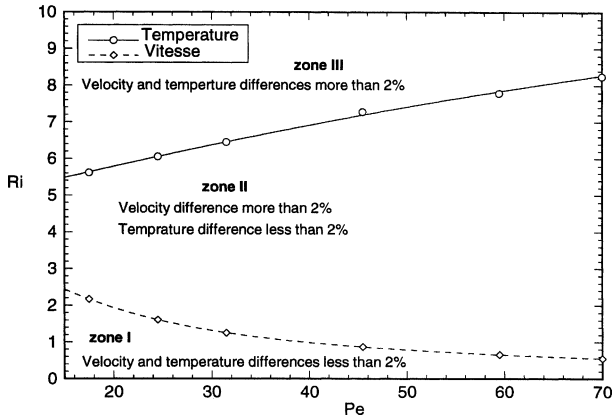

Figure 14. Effects of upstream diffusion for $Pr = 0.7$.

4. CONCLUSION

The results presented in this paper show that the flow field for laminar developing mixed convection with aiding buoyancy in vertical tubes is influenced by the ratio of the heating zone length to tube diameter and by the flow parameters (the Prandlt, Reynolds and Grashof numbers). In particular, the values of these four non-dimensional parameters determine whether flow reversal occurs, whether the flow is developing or fully developed and whether upstream diffusion of heat and momentum are significant. Therefore they should all be taken into consideration when deciding on the use of an axially parabolic or fully elliptic model and on the application of the inlet boundary conditions at the beginning of the heated zone. The effects of the heating zone length have not been reported before.

Acknowledgements

The authors thank the Natural Sciences and Engineering Research Council of Canada, the Ministry of Intergovernmental Affairs of New Brunswick as well as the Ministère de l'Éducation du Québec for their financial support.

REFERENCES

[1] Hallman T.M., Combined forced and free laminar heat transfer in vertical tubes with uniform heat generation, ASME Transactions 78 (1956) 1831–1841.

[2] Choudhury D., Patankar S.V., Combined forced and free laminar convection in the entrance region of an inclined isothermal tube, ASME J. Heat Transfer 110 (1988) 901–909.

[3] Wang M., Tsuji T., Nagano Y., Mixed convection with flow reversal in the thermal entrance region of horizontal and vertical pipes, Internat. J. Heat Mass Transfer 37 (1994) 2305–2319.

[4] Ouzzane M., Galanis N., Effet de la conduction pariétale et de la répartition du flux thermique sur la convection mixte près de l'entrée d'une conduite inclinée, Internat. J. Therm. Sci. 38 (1999) 622–633.

[5] Kunugi T., Ichimiya K., Sakamoto Y., Effects of three dimensional flow separation due to non-uniform heating on laminar mixed convection in a square channel, in: Hewitt G.F. (Ed.), Proceedings 10th Internat. Heat Transfer Conf., Brighton UK, Vol. 5, 1994, pp. 501–506.

[6] Nesreddine H., Galanis N., Nguyen C.T., Effects of axial diffusion on laminar heat transfer with low Péclet numbers in the entrance region of thin vertical tubes, Numer. Heat Transfer 33 (1998) 247–266.

[7] Shah R.K., London A.L., Laminar Flow Forced Convection in Ducts, a Source Book for Compact Heat Exchanger Analytical Data, Academic Press, New York, 1978.

[8] Pagliarini G., Steady laminar heat transfer in the entry region of circular tubes with axial diffusion of heat and momentum, Internat. J. Heat Mass Transfer 32 (1989) 1037–1052.

[9] Yao L.S., Is a fully developed and non-isothermal flow possible in a vertical pipe?, Internat. J. Heat Mass Transfer 30 (1987) 707–716.

[10] Bernier M., Baliga B.R., Visualization of upward mixed convection flows in vertical pipes using a thin semi-transparent gold-film heater and dye injection, Internat. J. Heat Fluid Flow 13 (1992) 241–249.

[11] Patankar S.V., Spalding D.B., A calculation procedure for heat, mass and momentum transfer in three-dimensional parabolic flows, Internat. J. Heat Mass Transfer 15 (1972) 1787–1806.

[12] Van Doormal J.P., Raithby G.D., Enhancement of the SIMPLE method for predicting incompressible fluid flows, Numer. Heat Transfer 7 (1984) 147–163.

[13] Zghal M., Effets de la convection naturelle sur le renversement de l'écoulement ascendant dans un conduit vertical, Mémoire M. Sci. A. Univ. de Sherbrooke, Québec, Canada, 1999.

[14] Kakac S., Yener Y., Convective Heat Transfer, CRC Press, Boca Raton, 1995.

[15] Kays W.M., Numerical solutions for laminar flow heat transfer in circular tubes, ASME Transactions 77 (1955) 1265–1274.

[16] Zeldin B., Schmidt F.W., Developing flow with combined forced-free convection in an isothermal vertical tube, ASME J. Heat Transfer 94 (1972) 211–223.

[17] Orfi J., Galanis N., Nguyen C.T., Laminar mixed convection in the entrance region of inclined pipes with high uniform heat fluxes, ASHRAE Transactions 104 (1998) 417–428.